REGULARIZING ENERGY AMONG TRAINING SAMPLES FOR OUT-OF-DISTRIBUTION GENERALIZATION

Anonymous authors
Paper under double-blind review

ABSTRACT

The energy-based model provides a unified framework for various learning models where an energy value is assigned to each configuration of random variables based on probability. Recently, different methods have been proposed to derive an energy value out of the logits of a classifier for out-of-distribution (OOD) detection or OOD generalization. However, these methods mainly focus on the energy difference between in-distribution and OOD data samples, neglecting the energy difference among in-distribution data samples. In this paper, we show that the energy among in-distribution data also requires attention. We propose to investigate the energy difference between in-distribution data samples. Both empirically and theoretically, we show that previous methods for subpopulation shift (*e.g.*, long-tail classification) such as data re-weighting and margin control apply implicit energy regularization and we provide a unified framework from the energy perspective. With the influence function, we further extend the energy regularization framework to OOD generalization scenarios where the distribution shift is more implicit compared to the long-tail recognition scenario. We conduct experiments on long-tail datasets, subpopulation shift benchmarks, and OOD generalization benchmarks to show the effectiveness of the proposed energy regularization method. The source code will be made publically available.

1 INTRODUCTION

Energy-based models (EBMs) LeCun et al. (2006); Ranzato et al. (2006; 2007) provide a unified theoretical framework for various learning models where an energy value is assigned to each configuration of random variables regarding its probability. Derived from the logits of a classifier, previous works show that a discriminative model is also an energy model Xie et al. (2016); Grathwohl et al. (2020) and use it for generative tasks. Inspired by this, the corresponding energy model is employed for OOD detection Liu et al. (2020); Bitterwolf et al. (2022); Wu et al. (2023). Out-of-distribution (OOD) data samples are detected by a higher energy value than in-distribution(IID) data samples due to the classifier's low probability of seeing out-of-distribution data samples. Recent work Xie et al. (2022) also minimizes the distance of energy distribution between the source domain and target domain to enhance the performance in domain adaptation. However, these previous works mainly focus on the energy difference between IID data and OOD data, neglecting the energy difference between in-distribution data samples.

In this paper, we propose to investigate the energy difference between in-distribution data samples (training data samples) and regularize the energy on training samples to boost the OOD generalization performance. From the energy regularization perspective, we both empirically and theoretically show that long-tail recognition methods Wang et al. (2017); Zhou et al. (2018); Liu et al. (2019); Zhong et al. (2019); He et al. (2021); Zhong et al. (2021) (a special case of sub-population shift Cai et al. (2021); Koh et al. (2021)) such as reweighting data Zhang et al. (2018); Zhao et al. (2019); Ye et al. (2020); Hsieh et al. (2021) or controlling the classification margin Cao et al. (2019) could be regarded as an implicit regularization on the energy value of training samples. For domain generalization, a main branch of works focuses on invariant risk minimization Chang et al. (2020); Creager et al. (2021); Lin et al. (2021), which regularizes the risk across different training domains to learn an invariant classifier. While the energy value is unrelated to the risk, we show that regularizing energy value across training domains could also improve the OOD generalization and is orthogonal to the methods for invariant risk minimization. We propose an energy regularization method and verify

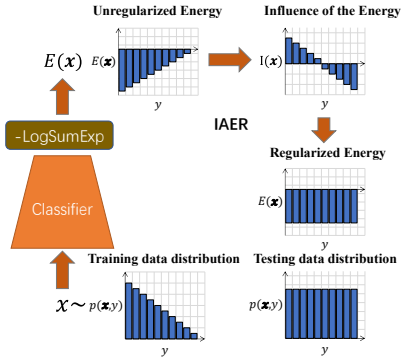

Figure 1: Illustration of our proposed Influence-Aware Energy Regularization (IAER). We quantify the influence of energy regularization and apply regularization accordingly.

Previous method	Differences between previous method and our method
Energy-based OOD detection	Previous works using energy to deal with OOD mainly focus on the energy difference between OOD data and in-distribution data, neglecting the energy difference between in-distribution data samples themselves.
Data re-weighting and margin control	These methods implicitly affect the energy value of in-distribution data. We provide a unified framework for them.
Invariant Risk Minimization	These methods propose regularizing the risk among training domains. Instead of focusing on the risk, we propose an orthogonal method that regularizes the energy among training domains.

Table 1: The relationship between previous works and ours

its effectiveness on tasks in long-tail classification, subpopulation shift, and domain generalization. Other empirical findings regarding the energy distribution of training data samples are provided. **We summarize the contributions of this paper in the following:**

- Besides the extensive research for OOD detection and OOD generalization focusing on the energy difference between out-of-distribution data and in-distribution data Liu et al. (2020); Bitterwolf et al. (2022); Wu et al. (2023); Xie et al. (2022), to the best of our knowledge, we are the first to call for attention to the energy difference between in-distribution data samples.
- We theoretically show that data re-weighting and margin control, the two branches of methods proposed for long-tail classification (a case for subpopulation shift) could be unified as implicit energy regularization among in-distribution data samples.
- We propose a method namely influence aware energy regularization to regularize energy among training domains to boost the model performance on OOD generalization.

2 Related Works

Energy Based Learning. Energy-based models (EBMs) LeCun et al. (2006); Ranzato et al. (2006; 2007) provide a unified theoretical framework for various learning models. Recent works employ the energy function defined on discriminative models for other tasks *e.g.* generative learning or OOD detection. Xie et al. (2016) shows that a generative random field model can be derived from a discriminative neural network. While Grathwohl et al. (2020) finds that neural classifiers are also energy-based models for joint distribution and devises a hybrid model that acts as both discriminative and generative models. Liu et al. (2020) proposes to use the energy value to detect OOD samples, which has been theoretically proved Bitterwolf et al. (2022) to be equal to training an additional binary discriminator. Recent work Xie et al. (2022) minimizes the distance of energy distribution between the source domain and target domain to enhance the performance in domain adaptation (see Wang & Deng (2018) and the references therein). However, these previous works focus on the energy difference between in-distribution data and out-of-distribution data, and we show that the energy difference between in-distribution data points could influence the generalization of the classifier.

Long-Tail Recognition. Long-tail recognition has drawn increasing attention Wang et al. (2017); Zhou et al. (2018); Liu et al. (2019); Zhong et al. (2019); He et al. (2021); Zhong et al. (2021) due to the pervasiveness of the imbalanced data in real-world scenarios. Most methods could be divided into three categories: re-sampling the data, re-weighting the loss, and transfer learning. For re-sampling, various methods have been proposed to re-sample the dataset to achieve a more balanced data distribution Chawla et al. (2002); Estabrooks et al. (2004); Han et al. (2005); Liu et al. (2009);

Shen et al. (2016); Liu et al. (2019); Wang et al. (2020); Kang et al. (2020); Zhang & Pfister (2021). As for re-weighting, re-weighting methods assign different losses to different classes Zhang et al. (2018); Zhao et al. (2019); Ye et al. (2020); Hsieh et al. (2021) or different data samples Lin et al. (2017); Ren et al. (2018); Shu et al. (2019) to achieve a more balanced performance on each class. Specifically, LDAM Cao et al. (2019) proposes a distribution aware loss that enlarges the margin to less frequent (tail) classes.

Subpopulation Shift. Subpopulation Shift focuses on changing the proportion of some subpopulations Cai et al. (2021); Koh et al. (2021), where subpopulations refer to subsets of a data domain divided by certain attributes. A conventional setting defines subpopulations as the product of attributes and classes Geirhos et al. (2020). In fact, long-tail recognition is a special case of subpopulation shift. Similar to long-tail classification, models tend to learn spurious features when minimizing overall loss, resulting in poor performance on minority subpopulations DeGrave et al. (2021); Joshi et al. (2022). A wide array of methods has been developed, some focusing on scenarios where attributes are known Gowda et al. (2021); Izmailov et al. (2022); Menon et al. (2020); Nam et al. (2022); Sagawa et al. (2019); Yao et al. (2022), while others investigate cases where attributes are unknown Creager et al. (2021); Han et al. (2022); Idrissi et al. (2022); Liu et al. (2021a).

Domain Generalization. Specifically, domain generalization (DG) Blanchard et al. (2011) aims to train a model using data from a single or multiple source domain that would generalize well to any out-of-distribution(OOD) target domains. Various methods have been proposed to tackle the domain generalization problem including learning domain-invariant representations Muandet et al. (2013); Li et al. (2018b;c), augmenting the data Zhou et al. (2020); Yan et al. (2020) and applying meta-learning to domain generalization Li et al. (2018a); Balaji et al. (2018). Some of the methods propose regularization strategies designed based on heuristics that surpass the predictive power of an auxiliary CNN implemented as a stack of 1×1 convolution layers Wang et al. (2019) or mask out the features with large gradients Huang et al. (2020). See Wang et al. (2021); Zhou et al. (2021) for a comprehensive survey.

3 Associating Methods in Long-tail Recognition With Training Energy Regularization

Various methods for long-tail recognition Wang et al. (2017); Zhou et al. (2018); Liu et al. (2019); Zhong et al. (2019); He et al. (2021); Zhong et al. (2021) (a case of subpopulation shift Cai et al. (2021); Koh et al. (2021)) have been proposed with different motivations. In this section, we show that these different long-tail recognition methods implicitly change the training energy and that energy regularization among training data samples unifies two different branches of long-tail recognition methods (reweighting Zhang et al. (2018); Zhao et al. (2019); Ye et al. (2020); Hsieh et al. (2021) and margin control Cao et al. (2019)).

3.1 Methods for Long-tail Recognition are Implicit Energy Regularization

For a K-class classification problem, a parameterized classifier $f_\theta : \mathbb{R}^D \to \mathbb{R}^K$ maps data point $\mathbf{x} \in \mathbb{R}^D$ to K real-valued logits where θ is the trainable parameter. For a data point $\mathbf{x}$ and its corresponding label y, the loss for the parameter θ is defined as $\mathcal{L}(\mathbf{x}, y, \theta)$. Energy-based model LeCun et al. (2006); Grathwohl et al. (2020) $E(\mathbf{x}) : \mathbb{R}^D \to \mathbb{R}$ maps each data point $\mathbf{x}$ to a single, non-probabilistic scalar called the energy, where the energy value could be turned to a probability as:

$$p(\mathbf{x}) = \frac{e^{-E(\mathbf{x})/T}}{\int_{\mathbf{x}'} e^{-E(\mathbf{x}')/T}}. \tag{1}$$

For classifier f_θ, the logits are typically converted to a normalized probability distribution with the Softmax function: $\bar{p}_\theta(y|\mathbf{x}) = \frac{\exp(f_\theta(\mathbf{x})[y])}{\sum_{y'} \exp(f_\theta(\mathbf{x})[y'])}$, where $f(\mathbf{x})[y]$ represents the logit corresponding to the y-th class. The joint distribution of data $\mathbf{x}$ and label y could be defined as $\bar{p}_\theta(\mathbf{x}, y) = \frac{\exp(f_\theta(\mathbf{x})[y])}{Z(\theta)}$ where $Z(\theta)$ is unknown normalizing constant. By marginalizing out y, the unnormalized density model for $\mathbf{x}$ is $\bar{p}_\theta(\mathbf{x}) = \sum_{y'} \bar{p}_\theta(\mathbf{x}, y') = \frac{\sum_{y'} \exp(f_\theta(\mathbf{x})[y'])}{Z(\theta)}$. Therefore the energy at data point $\mathbf{x}$

regarding to $\bar{p}_\theta(\mathbf{x})$ could be defined as:

$$E_\theta(\mathbf{x}) = -\log \sum_{y'} \exp\left(f_\theta(\mathbf{x})[y']\right). \tag{2}$$

The energy defined on classifiers is firstly introduced for generative tasks Xie et al. (2016); Grathwohl et al. (2020), where a classifier could be treated as an EBM and used for image generation. The energy of classifiers is also used for OOD detection Liu et al. (2020); Bitterwolf et al. (2022); Wu et al. (2023) where unseen data samples (OOD samples) generally have higher energy.

Similar to the OOD detection scenario, the energy is lower on sub-populations with large amounts of data in the sub-population shift scenarios Cai et al. (2021); Koh et al. (2021) (*e.g.* the classes having much more data samples than other classes in long-tail classification). In this section, taking long-tail recognition as a typical and clear case of sub-population shift, we show that various methods proposed to tackle the long-tail recognition problem apply implicit energy regularization.

Data resampling or re-weighting Zhang et al. (2018); Zhao et al. (2019); Ye et al. (2020); Hsieh et al. (2021) is one of the main branches of methods for long-tail recognition. By assigning different weights to different classes or sampling the data from the minor classes with little data more often, these methods encourage the model to reduce the loss of training data samples from the minor classes. Similar to the OOD detection scenario, the energy on more frequently trained data would be lower, which implicitly regularizes the energy on training data samples. Cao et al. (2019) also proposes margin control for better long-tail recognition performance. The classification margin is the difference between the logit of the ground-truth label and the largest logit of non-ground-truth labels. By controlling the classification margin to be larger for data samples from minor classes, the method prevents the model from misclassifying minor classes and improves the model performance. By controlling the margin, the logits are enlarged for the data samples from minor classes, which also implicitly regularizes the energy and encourages a more uniform energy distribution between the minor and major classes.

In Fig. 2, we train ResNet-32 on CIFAR10-LT and CIFAR100-LT following Cao et al. (2019) and report the average energy of each class. Generally, for the models trained with ERM Vapnik (1998), the energy is lower on the classes with more data samples indicating a larger probability $p(\mathbf{x})$ (Pearson Correlation Coefficient is at -0.74 on CIFAR10-LT and -0.60 on CIFAR100-LT). This phenomenon is because the model is trained to give lower energy (corresponding to higher $\bar{p}(\mathbf{x})$) to the frequently trained data, which has been utilized to detect OOD samples Liu et al. (2020). On the other hand, the models trained with LDAM have a more uniform energy distribution among classes (Pearson Correlation Coefficient is at -0.26 on CIFAR10-LT and 0.16 on CIFAR100-LT. It empirically shows how the margin control implicitly affects the energy among training samples. In the next section, we theoretically unify the sample re-weighting and margin control in energy regularization.

As a special case of sub-population shift, the long-tail recognition shows a clear probability shift as the probability of data samples from some classes is higher. Methods such as re-weighting or margin control implicitly affect the energy, pushing the $p(\mathbf{x})$ predicted by the model closer to following a uniform distribution, the ground truth distribution in the test set.

3.2 Unifying Reweighting and Margin Control in Energy Regularization

To deal with the imbalanced distribution among different classes in long-tail recognition, many previous works resort to assigning different weights to samples from different classes Zhang et al. (2018); Zhao et al. (2019); Ye et al. (2020); Hsieh et al. (2021), while other works such as LDAM Cao et al. (2019) adjust the margin to the decision boundary for different classes. In this section, we show that energy regularization actually unifies both data re-weighting and margin control. Starting with a cross-entropy loss, for a data sample $\mathbf{x}$ and the ground truth label y, we have

$$\mathcal{L}_{ce}(\mathbf{x}, y, \theta) = -\log \frac{\exp(f_\theta(\mathbf{x})[y])}{\sum_{y'} \exp(f_\theta(\mathbf{x})[y'])} = -f_\theta(\mathbf{x})[y] - E_\theta(\mathbf{x}) \tag{3}$$

Adding an energy regularization with coefficient $\hat{\beta}_\mathbf{x}$ regarding the input $\mathbf{x}$, we have

$$\mathcal{L}_{ce}(\mathbf{x}, y, \theta) + \hat{\beta}_\mathbf{x} \cdot E_\theta(\mathbf{x}) = -f_\theta(\mathbf{x})[y]) - (1 - \hat{\beta}_\mathbf{x}) \cdot E_\theta(\mathbf{x}) \tag{4}$$

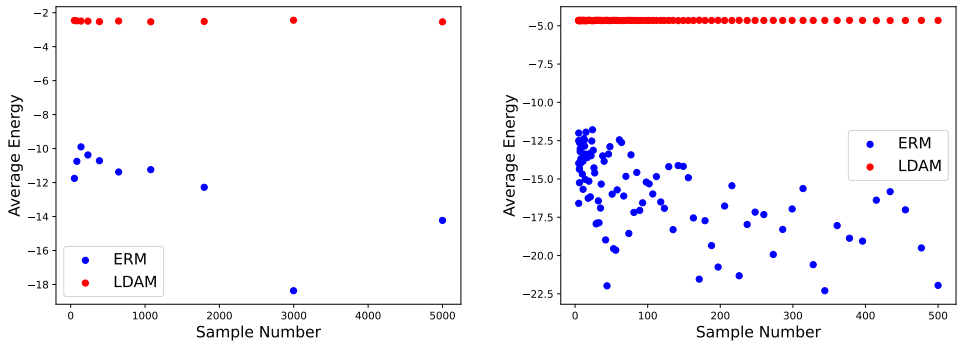

(a) CIFAR10-LT (b) CIFAR100-LT

Figure 2: Average energy of each class of ResNet-32 trained on CIFAR10-LT and CIFAR100-LT. We follow the hyper-parameter setting in Cao et al. (2019) to train models. Each dot corresponds to a class. The model trained by ERM has a biased energy distribution, where energy is generally lower for the class with more data. (The Pearson correlation coefficient is -0.74 on CIFAR10-LT and -0.60 on CIFAR100-LT.) As for the model trained with LDAM Cao et al. (2019), the average energy of different classes is nearly identical. (The Pearson correlation coefficient is -0.26 on CIFAR10-LT and 0.16 on CIFAR100-LT.) The results empirically indicate the LDAM is actually an implicit energy regularization and levels the energy on samples from different classes.

Then the gradient of the loss is:

$$\frac{\partial[\mathcal{L}_{ce}(\mathbf{x},y,\theta)+\hat{\beta}_{\mathbf{x}}\cdot E_\theta(\mathbf{x})]}{\partial\theta}=\left[(1-\hat{\beta}_{\mathbf{x}})\cdot\bar{p}(y|\mathbf{x})-1\right]\frac{\partial f_\theta(\mathbf{x})[y]}{\partial\theta}+(1-\hat{\beta}_{\mathbf{x}})\sum_{y'\neq y}\bar{p}(y'|\mathbf{x})\cdot\frac{\partial f_\theta(\mathbf{x})[y']}{\partial\theta}. \tag{5}$$

When $\hat{\beta}_{\mathbf{x}}\neq 1$, we could further derive the gradient as:

$$\frac{\partial\mathcal{L}(\mathbf{x},y,\theta)}{\partial\theta}=(1-\hat{\beta}_{\mathbf{x}})\cdot\left[\bar{p}(y|\mathbf{x})-\frac{1}{1-\hat{\beta}_{\mathbf{x}}}\right]\frac{\partial f_\theta(\mathbf{x})[y]}{\partial\theta}+(1-\hat{\beta}_{\mathbf{x}})\cdot\sum_{y'\neq y}\bar{p}(y'|\mathbf{x})\cdot\frac{\partial f_\theta(\mathbf{x})[y']}{\partial\theta}. \tag{6}$$

where $\mathcal{L}(\mathbf{x},y,\theta)=\mathcal{L}_{ce}(\mathbf{x},y,\theta)+\hat{\beta}_{\mathbf{x}}\cdot E_\theta(\mathbf{x})$. As shown in Eq. 6, the influence of energy regularization is twofold: adjusting the margin and reweighting data points. The weight for each data point is $1-\hat{\beta}_{\mathbf{x}}$. As for the margin, the margin is defined as $f_\theta(x)[y]-max_{j\neq y}f_\theta(x)[j]$ in Cao et al. (2019). In Eq. 6, the coefficient of the gradient $\frac{\partial f_\theta(\mathbf{x})[y]}{\partial\theta}$ is changed from $\bar{p}(y|\mathbf{x})-1$ to $\bar{p}(y|\mathbf{x})-\frac{1}{1-\hat{\beta}_{\mathbf{x}}}$. When $0<\hat{\beta}_{\mathbf{x}}<1$, the energy regularization enlarges the margin by pushing down the coefficient of $\frac{\partial f_\theta(\mathbf{x})[y]}{\partial\theta}$ and down-weights the data point $\mathbf{x}$ with coefficient $(1-\hat{\beta}_{\mathbf{x}})$. When $\hat{\beta}_{\mathbf{x}}<0$, the regularizer reduces the margin and up-weights the data $\mathbf{x}$ with coefficient $(1-\hat{\beta}_{\mathbf{x}})$. Therefore, we theoretically show that regularizing energy is actually a combination of data reweighting and margin control unifying two different branches of methods in long-tail recognition.

4 Regularizing Energy for OOD Generalization

In Sec. 3, we show that long-tail recognition methods such as LDAM Cao et al. (2019) implicitly regularize the energy. In this section, we want to extend the energy regularization to a more general OOD generalization scenario. In the long-tail recognition scenario, the disparity of data amount between different classes is known, guiding the data re-weighting or margin control. Since the distribution shift in the OOD generalization scenario is more implicit, it requires a method to determine the energy regularization coefficient $\hat{\beta}_{\mathbf{x}}$. Note that energy regularization is orthogonal to the previous methods regularizing the risk among different domains the reasons are as follows.

Motivation: The energy correlates to the probability of a data sample $p(\mathbf{x})$ predicted by the model. Similar to the long-tail recognition scenario, we wish the predicted probability to be close to the

actual probability in the test domain. While we have no way of knowing the test data distribution, the least we can do is to prevent the model from being over-confident (*i.e.* expect the unexpected). Note that the energy does not correspond to the prediction of the classifier (Remark 4.1), which is the reason most previous works overlook the energy disparity between training data samples and also make the energy regularization orthogonal to previous works focusing on regularizing the risk Chang et al. (2020); Creager et al. (2021); Lin et al. (2021).

Remark 4.1. ***[Arbitrary Energy]*** *Consider $\forall(\mathbf{x}, y) \in D_{train}$ and a classifier f_θ. For $\forall \mathcal{E} \in \mathbb{R}$, there exists a classifier g_η that satisfy*

$$\begin{aligned} \bar{p}_\theta(y|\mathbf{x}) &= \bar{p}_\eta(y|\mathbf{x}), \\ E_\eta(\mathbf{x}) &= \mathcal{E}. \end{aligned} \tag{7}$$

where $\bar{p}_\theta(y|\mathbf{x})$ and $\bar{p}_\eta(y|\mathbf{x})$ is the conditional probability predicted by f_θ and g_η respectively while $E_\eta(\mathbf{x})$ is the energy value of g_η on data point $\mathbf{x}$.

4.1 Determining Energy Regularization Coefficient via Influence Function

The difference between a typical OOD generalization scenario and long-tail recognition is that the distribution shift is implicit. One of the main challenges in applying energy regularization is determining the coefficient β in Eq. 5 as we do not know the testing data distribution. In this paper, we introduce the influence function to determine the coefficient β. Influence function Cook & Weisberg (1982) was used to determine the influence of training data samples on the model performance Koh & Liang (2017). Similar to that in Koh & Liang (2017), given a training set with n data points $D_{train} = \{(\mathbf{x}_1, y_1), (\mathbf{x}_2, y_2), \cdots (\mathbf{x}_n, y_n)\}$, the optimal parameter for empirical risk is given by $\hat{\theta} \overset{def}{=} \arg\min_\theta \frac{1}{n}\sum_{i=1}^n \mathcal{L}(\mathbf{x}_i, y_i, \theta)$. When we add an energy regularization on a training data point $(\mathbf{x}, y)$ with a small ϵ, the new optimal parameter becomes $\hat{\theta}_{\epsilon,(\mathbf{x},y)} = \arg\min_\theta(\frac{1}{n}\sum_{i=1}^n \mathcal{L}(\mathbf{x}_i, y_i, \theta) + \epsilon E_\theta(\mathbf{x}))$. Assume that the empirical risk is twice-differentiable and strictly convex w.r.t. θ, the influence function provides the influence of the energy regularization on $(\mathbf{x}, y)$:

$$\mathcal{I}_{\hat{\theta}}(\mathbf{x}, y) \overset{def}{=} \frac{\mathrm{d}\hat{\theta}_{\epsilon,(\mathbf{x},y)}}{\mathrm{d}\epsilon}|_{\epsilon=0} = -H_{\hat{\theta}}^{-1}\nabla_\theta E_\theta(\mathbf{x}). \tag{8}$$

where $H_{\hat{\theta}} = \frac{1}{n}\sum_{i=1}^n \nabla_\theta^2 \mathcal{L}(\mathbf{x}_i, y_i, \hat{\theta})$ is the Hessian matrix. Using the chain rule, the influence on the loss at a validation point $(\mathbf{x}_{va}, y_{va})$ is:

$$\begin{aligned} \mathcal{I}_{(\mathbf{x}_{va},y_{va})}(\mathbf{x}, y) &\overset{def}{=} \nabla_\theta \mathcal{L}(\mathbf{x}_{va}, y_{va}, \hat{\theta})^\top \frac{\mathrm{d}\hat{\theta}_{\epsilon,z}}{\mathrm{d}\epsilon}|_{\epsilon=0} \\ &= -\nabla_\theta \mathcal{L}(z_{test}, \hat{\theta})^\top H_{\hat{\theta}}^{-1}\nabla_\theta E_\theta(\mathbf{x}). \end{aligned} \tag{9}$$

This definition is similar to that in Koh & Liang (2017). Based on our devised influence function of energy, we propose a principled method that introduces **I**nfluence **A**ware **E**nergy **R**egularization (we refer to it as **IAER**). It firstly calculates the average influence of energy regularization on a validation set $D_{val} = \{(\mathbf{x}_i^{val}, y_i^{val})\}_{i=1}^m$ for each training data point. To fairly compare with previous works, we take subsets of the training set as the validation set without introducing any additional data. The average influence of energy regularization on the validation set is

$$\mathcal{I}_{val}(\mathbf{x}_i) = \frac{1}{m}\sum_{j=1}^m \mathcal{I}_{(\mathbf{x}_j^{val}, y_j^{val})}(\mathbf{x}_i) \tag{10}$$

To reduce the loss on the validation set, we increase the energy on the data points with a positive influence of energy regularization and decrease the energy on those with a negative influence. Therefore, we finetune the model with energy penalties determined by the corresponding influence value. The coefficient $\beta_{\mathbf{x}_i}$ for data $\mathbf{x}_i$ is

$$\beta_{\mathbf{x}_i} = -\gamma \cdot \mathcal{I}_{val}(\mathbf{x}_i)/\mathcal{I}_{val}^{max}. \tag{11}$$

Here $\mathcal{I}_{val}^{max}$ is the maximum absolute value of influence value over the train set D_{train}, and we set the hyperparameter $0 < \gamma < 1$, by which we make sure that the energy regularization does not interfere the optimization on cross-entropy.

Table 2: Average testing accuracy (%) of our method on Imbalanced CIFAR10/CIFAR100.

Dataset	Imbalanced CIFAR10				Imbalanced CIFAR100			
Imbalance type	long-tailed Cui et al. (2019)		step Buda et al. (2018)		long-tailed Cui et al. (2019)		step Buda et al. (2018)	
Imbalance Ratio	100	10	100	10	100	10	100	10
ERM Cao et al. (2019)	70.36	86.61	63.30	84.27	38.32	56.59	38.55	54.70
LDAM-DRW Cao et al. (2019)	77.16	87.62	75.36	87.42	42.04	56.67	**45.36**	56.84
ERM + IAER	75.83	87.02	71.33	85.62	39.60	**57.59**	39.12	55.10
LDAM-DRW + IAER	**78.37**	**87.72**	**75.89**	**87.70**	**42.81**	56.67	44.61	**56.9**

4.2 Experiments With IAER in Different Scenario

4.2.1 Long-tail Recognition

We first conduct experiments on the long-tail recognition scenario to test our energy regularization method. We evaluate IAER on the imbalanced version of CIFAR10, CIFAR100 Cui et al. (2019) and ImageNet-LT Liu et al. (2019) that are artificially created with class imbalance and iNaturalist 2018 Van Horn et al. (2018), a naturally long-tailed dataset. Experiments are conducted on imbalanced CIFAR following Cao et al. (2019) and on ImageNet-LT following Kang et al. (2020). For a fair comparison, the validation set used to calculate the influence function is sampled from the training set, and the models are not exposed to testing data during training.

Results on CIFAR. We evaluate IAER with ResNet-32 trained by: 1) Empirical risk minimization (ERM): with equal weight for each training data, and the model is trained to minimize the cross-entropy. 2) LDAM-DRW Cao et al. (2019): LDAM introduces a label-distribution aware margin loss, enlarging the decision while DRW applies re-weighting or re-sampling after the last learning rate decay. Since ERM is the basic training algorithm and a typical baseline while LDAM-DRW achieves SOTA on imbalanced CIFAR datasets, we take these two methods as baselines.

CIFAR10 and CIFAR100 both contain $50,000$ images in training and $10,000$ images in testing with 10 and 100 classes, respectively. We construct the imbalanced version of CIFAR10 and CIFAR100 by reducing the number of images for each class. Two types of imbalance are considered: long-tailed imbalance Cui et al. (2019) and step imbalance Buda et al. (2018). For long-tailed imbalance, the number of data points follows an exponential decay across different classes. For step imbalance, data points in half of the classes are reduced to the same number while the number of data points in the other classes remains the same.

As shown in Table 2, our method could effectively boost the testing performance after only 5 epochs. The more imbalanced the IAER is, the more effective it is. Notably, IAER could greatly improve the ERM pre-trained model. For instance, IAER reduces the testing error of the ERM pre-trained model for 5.47% (from 29.64% to 24.17%) on long-tailed CIFAR10 with the imbalance ratio at 100. For CIFAR100, IAER also improves the testing performance for the ERM pre-trained model and improves the LDAM-DRW pre-trained model on long-tailed CIFAR100 with the imbalance ratio at 100 and step-imbalanced CIFAR100 with the imbalance ratio at 10. However, the improvement in imbalanced CIFAR100 brought by our IAER is much smaller than that of imbalanced CIFAR10. We conjecture that the calculated influence of energy regularization on our sampled validation set for CIFAR100 is less accurate since the number of images per class in CIFAR100 is much smaller than that of CIFAR10 *e.g.* only 5 images for the least frequent class when imbalance ratio is 100.

Results on ImageNet-LT And iNaturalist 2018. We evaluate IAER with ResNeXt-50 Xie et al. (2017) pre-trained by the techniques and protocols proposed in Kang et al. (2020) where each model is divided into two parts: backbone and linear classifier. The protocol includes (1) Classifier Re-training (cRT): employ the backbone trained with ERM and retrain the linear classifier with the class balance sampling method. (2) Learnable Weight Scaling (LWS): Rescale the weight of the classifier for each class by a rescaling factor learned with the class balance sampling method as in cRT. ImageNet-LT Liu et al. (2019) is artificially truncated from ImageNet Deng et al. (2009), where the label distribution follows a long-tailed distribution. It has 1000 classes, and the number of images per class ranges from 1280 to 5. iNaturalist 2018 Van Horn et al. (2018) is a real-world, long-tailed dataset with 8142 classes. We follow Liu et al. (2019) and report the testing accuracy on three kinds of class sets: *Many-shot* (over 100 images), *Medium-shot* ($20 \sim 100$ images) and *Few-shot* (less than 20 images). The testing accuracy on all classes is denoted as *All*.

Table 3: Experiments on ImageNet-LT and iNaturalist. The validation set for IAER is composed of images in the train set.

Dataset and model	ResNeXt-50 on ImageNet-LT				ResNet-152 on iNaturalist			
Method	Many	Median	Few	All	Many	Median	Few	All
cRT Kang et al. (2020)	61.8	46.2	27.4	49.6	75.9	71.9	69.1	71.2
cRT + IAER[Few]	61.0	45.6	**29.1**	49.3	76.1	71.6	**69.5**	71.2
cRT + IAER[Median]	58.5	**48.7**	26.0	49.4	75.8	**72.3**	68.0	71.0
cRT + IAER[Many]	**62.7**	44.5	26.9	49.1	**77.8**	69.9	66.5	69.4
LWS Kang et al. (2020)	60.2	47.2	30.3	49.9	74.3	72.4	71.2	72.1
LWS + IAER[Few]	60.1	47.1	**32.1**	**50.1**	74.4	72.4	**71.6**	**72.3**
LWS + IAER[Median]	58.1	**49.0**	30.3	50.0	74.5	**72.8**	70.9	72.2
LWS + IAER[Many]	**61.5**	45.5	30.1	49.6	**74.9**	72.6	71.0	72.2

Table 4: Experiment results for subpopulation shift conducted based on SubpopBench Yang et al. (2023) on CMNIST Arjovsky et al. (2019), MetaShift cats *vs.* dogs Liang & Zou (2022), NICO++ Zhang et al. (2023), Waterbirds Wah et al. (2011) and CivilComments Borkan et al. (2019).

Dataset and Method	ERM		ERM + IAER	
Metric	Mean	Worst	Mean	Worst
CMNIST	77.8	4.6	**78.1**	**14.3**
MetaShift	90.4	66.2	**90.6**	**67.7**
NICO++	82.0	30.0	**82.8**	**33.3**

Note that the minimum number of data points per class in the training set of iNaturalist is 2, which makes the possible class-balanced subset of the training set extremely small. Therefore, for ImageNet-LT and iNaturalist, we take images of *Many-shot*, *Medium-shot*, and *Few-shot* classes in the training set as the validation set, respectively. We employ the backbone provided by Kang et al. (2020) and finetune or retrain the classifier. For ImageNet-LT, we calculate the influence of energy regularization on the ResNeXt-50 pre-trained for 90 epochs and retrain the classifiers with IAER for 10 epochs. For iNaturalist 2018, we calculate the influence of energy regularization of the ResNet-152 pretrained for 200 epochs. The classifiers on the iNaturalist are retrained for 30 epochs with energy regularization. More details are in Appendix A.

As shown in Table 3, IAER[Few] means that the validation set used for calculating influence is composed of images of *few-shot* classes in the training set while IAER[Median] and IAER[Many] means the validation set is composed by *median-shot* classes and *many-shot* classes respectively. For ImageNet-LT and iNaturalist 2018, we could observe that the accuracy on the classes used to calculate the influence function is boosted *e.g.* IAER[Few] boosts the accuracy of the classifier on *few-shot* classes while IAER[Median] boosts the accuracy of the classifier on *median-shot* classes. LWS combined with IAER[Few] could improve the accuracy of the whole testing set.

4.2.2 Results for Subpopulation Shift

We follow SubpopBench Yang et al. (2023) to conduct experiments for subpopulation shift. Subpopulations are subgroups of a data domain divided based on certain features, and subpopulation shift is a type of distribution shift characterized by changes in the proportion of some subpopulations. The long-tail dataset could be seen as a special case of subpopulation shift. We conduct our experiments on widely used datasets in SubpopBench, including ColoredMNIST Arjovsky et al. (2019), MetaShift cats *vs.* dogs Liang & Zou (2022), NICO++ Zhang et al. (2023). For a fair comparison, we use the training set as the proxy validation set to calculate the influence function. For the model training, we follow the setting in SubpopBench. As shown in Table 4, both the mean accuracy and the worst accuracy are improved with our IAER.

4.2.3 Results for Domain Generalization

We follow DomainBed Gulrajani & Lopez-Paz (2021) to conduct experiments for domain generalization. DomainBed is a testbed for domain generalization. As Gulrajani & Lopez-Paz (2021) shows that ERM outperforms SOTAs by average performance on common benchmarks as evaluated in a consistent and realistic setting, we combine our method with ERM and take the algorithms

Table 5: Experiment results for domain generalization conducted on CMNIST Arjovsky et al. (2019), PACS Li et al. (2017) and VLCS Fang et al. (2013).(* means we use the results from Domainbed Gulrajani & Lopez-Paz (2021))

Method	CMNIST	PACS	VLCS
ERM Vapnik (1998)	51.5 ± 0.1	85.5 ± 0.1	77.4 ± 0.2
IRM Arjovsky et al. (2019)*	52.0 ± 0.1	83.5± 0.8	78.5 ± 0.5
GroupDRO Sagawa et al. (2019)*	52.0 ± 0.0	84.4 ± 0.8	76.7 ± 0.6
MLDG Li et al. (2018a)*	51.5 ± 0.1	84.9 ± 1.0	77.2 ± 0.4
CORAL Sun & Saenko (2016)	51.2 ± 0.1	86.1 ± 0.2	78.8 ± 0.6
SagNet Nam et al. (2021)	51.7 ± 0.0	86.3 ± 0.1	77.8 ± 0.5
ERM + IAER	51.9 ± 0.1	86.6 ± 0.1	78.5 ± 0.2

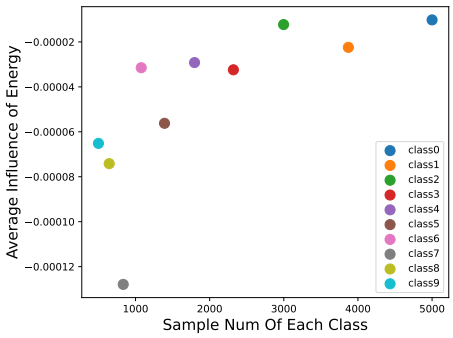

Figure 3: The average influence of energy regularization on CIFAR10-LT. Each dot represents a class, and the x-axis corresponds to the number of data samples in that class.

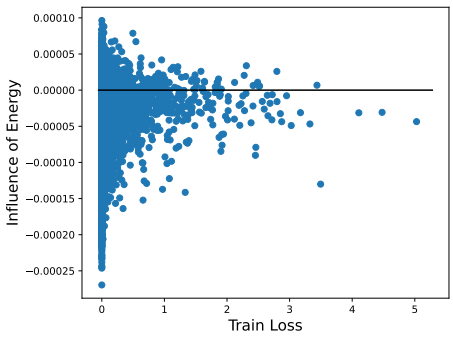

Figure 4: Influence of energy regularization and loss of each training data point (a dot in the plot) in long-tailed CIFAR10 for ResNet-32 trained with ERM.

implemented in DomainBed as baselines. Experiments are performed on benchmarks ColoredMNIST Arjovsky et al. (2019), PACS Li et al. (2017) and VLCS Fang et al. (2013).

As mentioned in Sec. 4.1, we take the training set as the validation set to calculate the influence function for a fair comparison. We follow the setting in DomainBed Gulrajani & Lopez-Paz (2021) to train the model. We demonstrate the results using training domain validation as model selection criteria which use a validation set sampled from the training domain for model selection. For each algorithm and testing domain, we conduct a random search of 5 trails. For more details, see Appendix A.

As shown in Table 5, our IAER could improve the accuracy on the test domain without the test domain information. This implies that regularizing energy on the training domains helps generalize the training domains to the testing domain. More results are in Appendix B.

5 Other Empirical Results

5.1 Average Influence of Energy Regularization on CIFAR10-LT

We plot the average influence of energy regularization of each class on CIFAR10-LT. As shown in Fig. 3, the average influence of energy regularization of different classes is positively correlated to the number of data points of the corresponding class (The Pearson's R is 0.70 for long-tailed CIFAR10 with imbalance ratio at 10). The lower the influence of the energy regularization, the lower the testing loss of the classifier would be after adding a positive energy regularization. It indicates that pushing down the energy value of data points of less frequent class and pulling up the energy value of data points of more frequent class would boost the testing performance *i.e.* pull up the predicted $\bar{p}(\mathbf{x})$ for less frequent class and push down the predicted $\bar{p}(\mathbf{x})$ for more frequent class. Since the probability density $p(\mathbf{x})$ of data points of less frequent class is much lower and the $p(\mathbf{x})$

Table 6: Time required to approximate the influence function on different datasets.

Model	Dataset	iteration	repeat times	time used
ResNet-32	CIFAR10	5000	10	718.20s
ResNeXt-50	ImageNet-LT	1000	10	8492.92s
ResNet-152	iNaturalist 2018	1000	10	9701.74s

of data points of more frequent class is much higher in the imbalanced training set compared to the testing set, it shows that pushing the predicted $\bar{p}(\mathbf{x})$ closer to the real $p(\mathbf{x})$ of the testing set would boost the testing performance. According to Sec. 3.2, our regularization method generally enlarges the margin and down-weights for the less frequent classes. On the other hand, it reduces the margin and up-weights for the more frequent classes.

5.2 Influence of Energy Regularization on Data Samples with Different Loss

To investigate the relationship between the influence of energy regularization and the loss on each training data point, we provide a scatter figure as in Fig. 4. Note that the influence of energy regularization on the data points of similar training loss ranges from positive to negative. The influence of energy regularization is not related to the training loss (Pearson's R is -0.04). This indicates that one could not predict the influence of energy regularization on the data point based on training loss. However, the range of the influence of energy regularization expands as the training loss decreases. Therefore, data points where energy regularization has a large influence are generally well-classified data points with low loss. As pointed out in Remark 4.1, the energy value is unstable during the training, *we conjecture that the un-regularized energy value of well-classified data points is one of the possible reasons for the overfitting of the classifier*.

5.3 Time Complexity Analysis for the Approximation of Influence Function

The main overhead of the proposed IAER is calculating the influence function of energy regularization. We calculate the influence function with stochastic estimation Cook & Weisberg (1982) following Koh & Liang (2017). We implement the calculation of the influence function based on the Python package for calculating the influence function Lo & Bae (2022). For imbalanced CIFAR10 and imbalanced CIFAR100, the influence function is calculated with stochastic estimation for 5000 iteration and averaged over 10 trails. For ImageNet-LT and iNaturalist, we calculate the influence function only on the classifier, and the influence function is calculated with stochastic estimation for 1000 iteration and averaged over 10 trails.

Since we approximate the influence function using stochastic approximation, the time used to calculate the influence function is determined by the choice of hyperparameters. We tested the time cost for calculating the influence function for ResNet-32 on CIFAR10 with Intel(R) Xeon(R) CPU E5-2678 v3 @ 2.50GHz and one GeForce RTX 2080Ti for 5000 iteration and averaged ten times. Approximating the influence function for a 5000 iteration takes 718.20s on average. As shown in Table 6, we report the time used to approximate the influence function on different datasets for different models with the same hardware settings.

6 Conclusion

In this paper, we propose to regularize the energy among training data samples. We first show that various methods for long-tail recognition implicitly apply energy regularization, which pushes the energy distribution close to the test distribution. We further propose an influence-aware energy regularization for various OOD generalization scenarios, such as subpopulation shift and domain generalization. The main limitation comes from the use of the influence function. First of all, it requires a validation set. In this paper, we use a subset of the training set as the validation set. Experimental results show that the choice of the validation set largely affects the performance of IAER. Secondly, as defined for convex loss functions, the influence function may not reflect the actual influence for neural networks. The approximation of the influence function is also a bottleneck, which is hard to converge and requires high computational cost. We hope the idea of regularizing energy on training data samples will innovate future works.

REFERENCES

Martín Arjovsky, Léon Bottou, Ishaan Gulrajani, and David Lopez-Paz. Invariant risk minimization. *CoRR*, abs/1907.02893, 2019.

Yogesh Balaji, Swami Sankaranarayanan, and Rama Chellappa. Metareg: Towards domain generalization using meta-regularization. In *NeurIPS*, pp. 1006–1016, 2018.

Julian Bitterwolf, Alexander Meinke, Maximilian Augustin, and Matthias Hein. Breaking down out-of-distribution detection: Many methods based on OOD training data estimate a combination of the same core quantities. In *ICML*, volume 162 of *Proceedings of Machine Learning Research*, pp. 2041–2074. PMLR, 2022.

Gilles Blanchard, Gyemin Lee, and Clayton Scott. Generalizing from several related classification tasks to a new unlabeled sample. In *NIPS*, pp. 2178–2186, 2011.

Daniel Borkan, Lucas Dixon, Jeffrey Sorensen, Nithum Thain, and Lucy Vasserman. Nuanced metrics for measuring unintended bias with real data for text classification. In *Companion proceedings of the 2019 world wide web conference*, pp. 491–500, 2019.

Mateusz Buda, Atsuto Maki, and Maciej A. Mazurowski. A systematic study of the class imbalance problem in convolutional neural networks. *Neural Networks*, 106:249–259, 2018.

Tianle Cai, Ruiqi Gao, Jason Lee, and Qi Lei. A theory of label propagation for subpopulation shift. In *International Conference on Machine Learning*, pp. 1170–1182. PMLR, 2021.

Kaidi Cao, Colin Wei, Adrien Gaidon, Nikos Aréchiga, and Tengyu Ma. Learning imbalanced datasets with label-distribution-aware margin loss. In *NeurIPS*, pp. 1565–1576, 2019.

Shiyu Chang, Yang Zhang, Mo Yu, and Tommi Jaakkola. Invariant rationalization. In *International Conference on Machine Learning*, pp. 1448–1458. PMLR, 2020.

Nitesh V. Chawla, Kevin W. Bowyer, Lawrence O. Hall, and W. Philip Kegelmeyer. SMOTE: synthetic minority over-sampling technique. *J. Artif. Intell. Res.*, 16:321–357, 2002.

R Dennis Cook and Sanford Weisberg. *Residuals and influence in regression*. New York: Chapman and Hall, 1982.

Elliot Creager, Jörn-Henrik Jacobsen, and Richard Zemel. Environment inference for invariant learning. In *International Conference on Machine Learning*, pp. 2189–2200. PMLR, 2021.

Yin Cui, Menglin Jia, Tsung-Yi Lin, Yang Song, and Serge J. Belongie. Class-balanced loss based on effective number of samples. In *CVPR*, pp. 9268–9277. Computer Vision Foundation / IEEE, 2019.

Alex J DeGrave, Joseph D Janizek, and Su-In Lee. Ai for radiographic covid-19 detection selects shortcuts over signal. *Nature Machine Intelligence*, 3(7):610–619, 2021.

Jia Deng, Wei Dong, Richard Socher, Li-Jia Li, Kai Li, and Li Fei-Fei. Imagenet: A large-scale hierarchical image database. In *CVPR*, pp. 248–255. IEEE Computer Society, 2009.

Andrew Estabrooks, Taeho Jo, and Nathalie Japkowicz. A multiple resampling method for learning from imbalanced data sets. *Comput. Intell.*, 20(1):18–36, 2004.

Chen Fang, Ye Xu, and Daniel N. Rockmore. Unbiased metric learning: On the utilization of multiple datasets and web images for softening bias. In *ICCV*, pp. 1657–1664. IEEE Computer Society, 2013.

Robert Geirhos, Jörn-Henrik Jacobsen, Claudio Michaelis, Richard Zemel, Wieland Brendel, Matthias Bethge, and Felix A Wichmann. Shortcut learning in deep neural networks. *Nature Machine Intelligence*, 2(11):665–673, 2020.

Sindhu CM Gowda, Shalmali Joshi, Haoran Zhang, and Marzyeh Ghassemi. Pulling up by the causal bootstraps: Causal data augmentation for pre-training debiasing. In *Proceedings of the 30th ACM International Conference on Information & Knowledge Management*, pp. 606–616, 2021.

Will Grathwohl, Kuan-Chieh Wang, Jörn-Henrik Jacobsen, David Duvenaud, Mohammad Norouzi, and Kevin Swersky. Your classifier is secretly an energy based model and you should treat it like one. In *ICLR*. OpenReview.net, 2020.

Ishaan Gulrajani and David Lopez-Paz. In search of lost domain generalization. In *ICLR*. OpenReview.net, 2021.

Hui Han, Wenyuan Wang, and Binghuan Mao. Borderline-smote: A new over-sampling method in imbalanced data sets learning. In *ICIC (1)*, volume 3644 of *Lecture Notes in Computer Science*, pp. 878–887. Springer, 2005.

Zongbo Han, Zhipeng Liang, Fan Yang, Liu Liu, Lanqing Li, Yatao Bian, Peilin Zhao, Bingzhe Wu, Changqing Zhang, and Jianhua Yao. Umix: Improving importance weighting for subpopulation shift via uncertainty-aware mixup. *Advances in Neural Information Processing Systems*, 35: 37704–37718, 2022.

Kaiming He, Xiangyu Zhang, Shaoqing Ren, and Jian Sun. Deep residual learning for image recognition. In *Proceedings of the IEEE conference on computer vision and pattern recognition*, pp. 770–778, 2016.

Yin-Yin He, Jianxin Wu, and Xiu-Shen Wei. Distilling virtual examples for long-tailed recognition. In *ICCV*, pp. 235–244. IEEE, 2021.

Ting-I Hsieh, Esther Robb, Hwann-Tzong Chen, and Jia-Bin Huang. Droploss for long-tail instance segmentation. In *AAAI*, pp. 1549–1557. AAAI Press, 2021.

Zeyi Huang, Haohan Wang, Eric P. Xing, and Dong Huang. Self-challenging improves cross-domain generalization. In *ECCV (2)*, volume 12347 of *Lecture Notes in Computer Science*, pp. 124–140. Springer, 2020.

Badr Youbi Idrissi, Martin Arjovsky, Mohammad Pezeshki, and David Lopez-Paz. Simple data balancing achieves competitive worst-group-accuracy. In *Conference on Causal Learning and Reasoning*, pp. 336–351. PMLR, 2022.

Pavel Izmailov, Polina Kirichenko, Nate Gruver, and Andrew G Wilson. On feature learning in the presence of spurious correlations. *Advances in Neural Information Processing Systems*, 35: 38516–38532, 2022.

Nitish Joshi, Xiang Pan, and He He. Are all spurious features in natural language alike? an analysis through a causal lens. *arXiv preprint arXiv:2210.14011*, 2022.

Bingyi Kang, Saining Xie, Marcus Rohrbach, Zhicheng Yan, Albert Gordo, Jiashi Feng, and Yannis Kalantidis. Decoupling representation and classifier for long-tailed recognition. In *ICLR*. OpenReview.net, 2020.

Pang Wei Koh and Percy Liang. Understanding black-box predictions via influence functions. In *ICML*, volume 70 of *Proceedings of Machine Learning Research*, pp. 1885–1894. PMLR, 2017.

Pang Wei Koh, Shiori Sagawa, Henrik Marklund, Sang Michael Xie, Marvin Zhang, Akshay Balsubramani, Weihua Hu, Michihiro Yasunaga, Richard Lanas Phillips, Irena Gao, et al. Wilds: A benchmark of in-the-wild distribution shifts. In *International Conference on Machine Learning*, pp. 5637–5664. PMLR, 2021.

Yann LeCun, Sumit Chopra, Raia Hadsell, M Ranzato, and F Huang. A tutorial on energy-based learning. *Predicting structured data*, 1(0), 2006.

Da Li, Yongxin Yang, Yi-Zhe Song, and Timothy M. Hospedales. Deeper, broader and artier domain generalization. In *ICCV*, pp. 5543–5551. IEEE Computer Society, 2017.

Da Li, Yongxin Yang, Yi-Zhe Song, and Timothy M. Hospedales. Learning to generalize: Meta-learning for domain generalization. In *AAAI*, pp. 3490–3497. AAAI Press, 2018a.

Haoliang Li, Sinno Jialin Pan, Shiqi Wang, and Alex C. Kot. Domain generalization with adversarial feature learning. In *CVPR*, pp. 5400–5409. Computer Vision Foundation / IEEE Computer Society, 2018b.

Ya Li, Xinmei Tian, Mingming Gong, Yajing Liu, Tongliang Liu, Kun Zhang, and Dacheng Tao. Deep domain generalization via conditional invariant adversarial networks. In *ECCV (15)*, volume 11219 of *Lecture Notes in Computer Science*, pp. 647–663. Springer, 2018c.

Weixin Liang and James Zou. Metashift: A dataset of datasets for evaluating contextual distribution shifts and training conflicts. *arXiv preprint arXiv:2202.06523*, 2022.

Tsung-Yi Lin, Priya Goyal, Ross B. Girshick, Kaiming He, and Piotr Dollár. Focal loss for dense object detection. In *ICCV*, pp. 2999–3007. IEEE Computer Society, 2017.

Yong Lin, Qing Lian, and Tong Zhang. An empirical study of invariant risk minimization on deep models. In *ICML 2021 Workshop on Uncertainty and Robustness in Deep Learning*, volume 1, pp. 7, 2021.

Evan Z Liu, Behzad Haghgoo, Annie S Chen, Aditi Raghunathan, Pang Wei Koh, Shiori Sagawa, Percy Liang, and Chelsea Finn. Just train twice: Improving group robustness without training group information. In *International Conference on Machine Learning*, pp. 6781–6792. PMLR, 2021a.

Weitang Liu, Xiaoyun Wang, John D. Owens, and Yixuan Li. Energy-based out-of-distribution detection. In *NeurIPS*, 2020.

Xu-Ying Liu, Jianxin Wu, and Zhi-Hua Zhou. Exploratory undersampling for class-imbalance learning. *IEEE Trans. Syst. Man Cybern. Part B*, 39(2):539–550, 2009.

Zhuoming Liu, Hao Ding, Huaping Zhong, Weijia Li, Jifeng Dai, and Conghui He. Influence selection for active learning. In *ICCV*, pp. 9254–9263. IEEE, 2021b.

Ziwei Liu, Zhongqi Miao, Xiaohang Zhan, Jiayun Wang, Boqing Gong, and Stella X. Yu. Large-scale long-tailed recognition in an open world. In *CVPR*, pp. 2537–2546. Computer Vision Foundation / IEEE, 2019.

Alston Lo and Juhan Bae. torch-influence, June 2022. URL `https://github.com/alstonlo/torch-influence`.

Aditya Krishna Menon, Ankit Singh Rawat, and Sanjiv Kumar. Overparameterisation and worst-case generalisation: friend or foe? In *International Conference on Learning Representations*, 2020.

Krikamol Muandet, David Balduzzi, and Bernhard Schölkopf. Domain generalization via invariant feature representation. In *ICML (1)*, volume 28 of *JMLR Workshop and Conference Proceedings*, pp. 10–18. JMLR.org, 2013.

Hyeonseob Nam, HyunJae Lee, Jongchan Park, Wonjun Yoon, and Donggeun Yoo. Reducing domain gap by reducing style bias. In *CVPR*, pp. 8690–8699. Computer Vision Foundation / IEEE, 2021.

Junhyun Nam, Jaehyung Kim, Jaeho Lee, and Jinwoo Shin. Spread spurious attribute: Improving worst-group accuracy with spurious attribute estimation. *arXiv preprint arXiv:2204.02070*, 2022.

Marc'Aurelio Ranzato, Christopher S. Poultney, Sumit Chopra, and Yann LeCun. Efficient learning of sparse representations with an energy-based model. In *NIPS*, pp. 1137–1144. MIT Press, 2006.

Marc'Aurelio Ranzato, Y-Lan Boureau, Sumit Chopra, and Yann LeCun. A unified energy-based framework for unsupervised learning. In *AISTATS*, volume 2 of *JMLR Proceedings*, pp. 371–379. JMLR.org, 2007.

Mengye Ren, Wenyuan Zeng, Bin Yang, and Raquel Urtasun. Learning to reweight examples for robust deep learning. In *ICML*, volume 80 of *Proceedings of Machine Learning Research*, pp. 4331–4340. PMLR, 2018.

Shiori Sagawa, Pang Wei Koh, Tatsunori B. Hashimoto, and Percy Liang. Distributionally robust neural networks for group shifts: On the importance of regularization for worst-case generalization. *CoRR*, abs/1911.08731, 2019.

Li Shen, Zhouchen Lin, and Qingming Huang. Relay backpropagation for effective learning of deep convolutional neural networks. In *ECCV (7)*, volume 9911 of *Lecture Notes in Computer Science*, pp. 467–482. Springer, 2016.

Jun Shu, Qi Xie, Lixuan Yi, Qian Zhao, Sanping Zhou, Zongben Xu, and Deyu Meng. Meta-weight-net: Learning an explicit mapping for sample weighting. In *NeurIPS*, pp. 1917–1928, 2019.

Baochen Sun and Kate Saenko. Deep CORAL: correlation alignment for deep domain adaptation. In *ECCV Workshops (3)*, volume 9915 of *Lecture Notes in Computer Science*, pp. 443–450, 2016.

Grant Van Horn, Oisin Mac Aodha, Yang Song, Yin Cui, Chen Sun, Alex Shepard, Hartwig Adam, Pietro Perona, and Serge Belongie. The inaturalist species classification and detection dataset. In *Proceedings of the IEEE conference on computer vision and pattern recognition*, pp. 8769–8778, 2018.

Vladimir Vapnik. *Statistical learning theory*. Wiley, 1998.

Catherine Wah, Steve Branson, Peter Welinder, Pietro Perona, and Serge Belongie. The caltech-ucsd birds-200-2011 dataset. 2011.

Haohan Wang, Zexue He, Zachary C. Lipton, and Eric P. Xing. Learning robust representations by projecting superficial statistics out. In *ICLR*. OpenReview.net, 2019.

Jindong Wang, Cuiling Lan, Chang Liu, Yidong Ouyang, and Tao Qin. Generalizing to unseen domains: A survey on domain generalization. In *IJCAI*, pp. 4627–4635. ijcai.org, 2021.

Mei Wang and Weihong Deng. Deep visual domain adaptation: A survey. *Neurocomputing*, 312: 135–153, 2018.

Tao Wang, Yu Li, Bingyi Kang, Junnan Li, Jun Hao Liew, Sheng Tang, Steven C. H. Hoi, and Jiashi Feng. The devil is in classification: A simple framework for long-tail instance segmentation. In *ECCV (14)*, volume 12359 of *Lecture Notes in Computer Science*, pp. 728–744. Springer, 2020.

Yu-Xiong Wang, Deva Ramanan, and Martial Hebert. Learning to model the tail. In *NIPS*, pp. 7029–7039, 2017.

Qitian Wu, Yiting Chen, Chenxiao Yang, and Junchi Yan. Energy-based out-of-distribution detection for graph neural networks. In *The Eleventh International Conference on Learning Representations, ICLR 2023, Kigali, Rwanda, May 1-5, 2023*. OpenReview.net, 2023.

Binhui Xie, Longhui Yuan, Shuang Li, Chi Harold Liu, Xinjing Cheng, and Guoren Wang. Active learning for domain adaptation: An energy-based approach. In *AAAI*, pp. 8708–8716. AAAI Press, 2022.

Jianwen Xie, Yang Lu, Song-Chun Zhu, and Ying Nian Wu. A theory of generative convnet. In *ICML*, volume 48 of *JMLR Workshop and Conference Proceedings*, pp. 2635–2644. JMLR.org, 2016.

Saining Xie, Ross B. Girshick, Piotr Dollár, Zhuowen Tu, and Kaiming He. Aggregated residual transformations for deep neural networks. In *CVPR*, pp. 5987–5995. IEEE Computer Society, 2017.

Shen Yan, Huan Song, Nanxiang Li, Lincan Zou, and Liu Ren. Improve unsupervised domain adaptation with mixup training. *CoRR*, abs/2001.00677, 2020.

Yuzhe Yang, Haoran Zhang, Dina Katabi, and Marzyeh Ghassemi. Change is hard: A closer look at subpopulation shift. In *International Conference on Machine Learning*, 2023.

Huaxiu Yao, Yu Wang, Sai Li, Linjun Zhang, Weixin Liang, James Zou, and Chelsea Finn. Improving out-of-distribution robustness via selective augmentation. In *International Conference on Machine Learning*, pp. 25407–25437. PMLR, 2022.

Han-Jia Ye, Hong-You Chen, De-Chuan Zhan, and Wei-Lun Chao. Identifying and compensating for feature deviation in imbalanced deep learning. *CoRR*, abs/2001.01385, 2020.

Xingxuan Zhang, Yue He, Renzhe Xu, Han Yu, Zheyan Shen, and Peng Cui. Nico++: Towards better benchmarking for domain generalization. In *Proceedings of the IEEE/CVF Conference on Computer Vision and Pattern Recognition*, pp. 16036–16047, 2023.

Yifan Zhang, Peilin Zhao, Jiezhang Cao, Wenye Ma, Junzhou Huang, Qingyao Wu, and Mingkui Tan. Online adaptive asymmetric active learning for budgeted imbalanced data. In *KDD*, pp. 2768–2777. ACM, 2018.

Zizhao Zhang and Tomas Pfister. Learning fast sample re-weighting without reward data. In *ICCV*, pp. 705–714. IEEE, 2021.

Peilin Zhao, Yifan Zhang, Min Wu, Steven C. H. Hoi, Mingkui Tan, and Junzhou Huang. Adaptive cost-sensitive online classification. *IEEE Trans. Knowl. Data Eng.*, 31(2):214–228, 2019.

Yaoyao Zhong, Weihong Deng, Mei Wang, Jiani Hu, Jianteng Peng, Xunqiang Tao, and Yaohai Huang. Unequal-training for deep face recognition with long-tailed noisy data. In *CVPR*, pp. 7812–7821. Computer Vision Foundation / IEEE, 2019.

Zhisheng Zhong, Jiequan Cui, Shu Liu, and Jiaya Jia. Improving calibration for long-tailed recognition. In *CVPR*, pp. 16489–16498. Computer Vision Foundation / IEEE, 2021.

Bolei Zhou, Àgata Lapedriza, Aditya Khosla, Aude Oliva, and Antonio Torralba. Places: A 10 million image database for scene recognition. *IEEE Trans. Pattern Anal. Mach. Intell.*, 40(6): 1452–1464, 2018.

Kaiyang Zhou, Yongxin Yang, Timothy M. Hospedales, and Tao Xiang. Learning to generate novel domains for domain generalization. In *ECCV (16)*, volume 12361 of *Lecture Notes in Computer Science*, pp. 561–578. Springer, 2020.

Kaiyang Zhou, Ziwei Liu, Yu Qiao, Tao Xiang, and Chen Change Loy. Domain generalization: A survey. *CoRR*, abs/2103.02503, 2021.

A EXPERIMENT DETAILS

A.1 DETAILS FOR THE CALCULATION OF INFLUENCE FUNCTION

The calculation of the influence function requires a validation set. For imbalanced CIFAR10 and CIFAR100, we sample data points of each class from the class-imbalanced training set to compose the validation set. The number of data points per class is determined by the minimum number of data points per class in the training set. For ImageNet-LT, since it has a validation split, we use the val split to calculate the influence function. For iNaturalist, since the minimum number of data points per class is APPall (2 images per class), we take the *few-shot* classes of the training set as the validation set.

We calculate the influence function with stochastic estimation Cook & Weisberg (1982) following Koh & Liang (2017). We implement the calculation of the influence function based on the Python package for calculating the influence function Lo & Bae (2022). For imbalanced CIFAR10 and imbalanced CIFAR100, the influence function is calculated with stochastic estimation for 5000 iteration and averaged over 10 trails. For ImageNet-LT and iNaturalist, we calculate the influence function only on the classifier, and the influence function is calculated with stochastic estimation for 1000 iteration and averaged over 10 trails.

A.2 DETAILS FOR THE EXPERIMENTS ON IMBALANCED DATASET

We follow the setting in Cao et al. (2019) to train ResNet-32 on the imbalanced CIFAR dataset and report the performance of the model at the final epoch. The model is trained for 200 epochs with SGD optimizer where the learning rate is at 0.1, momentum at 0.9, and weight decay at $2e-4$. The learning rate is decayed with factor 0.01 at 160-th epoch and 180-th epoch. For IAER, we finetune the model for 5 epochs with batch size at 128 and learning rate at $1e-4$.

For ImageNet-LT and iNaturalist 2018, we employ the pre-trained model provided in Kang et al. (2020) and follow the setting in it to finetune the ResNeXt-50 Xie et al. (2017) on ImgaeNet-LT and the ResNet-152 He et al. (2016) on iNaturalist 2018. For ImageNet-LT, the classifier is finetuned for 10 epochs with batch size at 512 and learning rate at 0.2. For iNaturalist, the classifier is finetuned for 30 epochs with batch size at 512 and learning rate at 0.2.

The γ in Eq. 9 is searched in $\{0.1, 0.5, 1, 10\}$ for CIFAR-LT and set to be 0.5 for ImageNet-LT and iNaturalist2018. When the absolute value of energy regularization is bigger than the cross-entropy loss the γ is set to be $\| \frac{\mathcal{L}_{ce}(\mathbf{x}_i^{tr}, y_i^{tr}, \theta)}{E_\theta(\mathbf{x}_i^{tr}) \cdot \mathcal{I}_{val}(\mathbf{x}_i^{tr}, y_i^{tr}) / \mathcal{I}_{val}^{max}} \|$

A.3 DETAILS FOR THE EXPERIMENTS FOR DOMAIN GENERALIZATION

We follow the setting in Gulrajani & Lopez-Paz (2021) to conduct experiments and use the training domain validation set to calculate the influence function. The γ in Eq. 9 is set to be 0.1. We employ the same training settings and hyperparameters implemented in Gulrajani & Lopez-Paz (2021).

A.4 COMPARISON BETWEEN THE INFLUENCE OF THE CROSS-ENTROPY AND THE INFLUENCE OF THE ENERGY.

The influence function of the cross-entropy has been widely used in data valuation Koh & Liang (2017) and active learning Liu et al. (2021b). As shown in Fig. 5, the influence of the cross-entropy and the influence of the energy do not correlate with each other. The influence function of the cross-entropy as in previous works Koh & Liang (2017); Liu et al. (2021b) evaluates the influence of reweighting the data points. As for the influence function of the energy, we focus on the influence of the energy regularization, which acts as reweighting and margin control. Therefore there are fundamental differences between the influence of the cross-entropy and that of the energy.

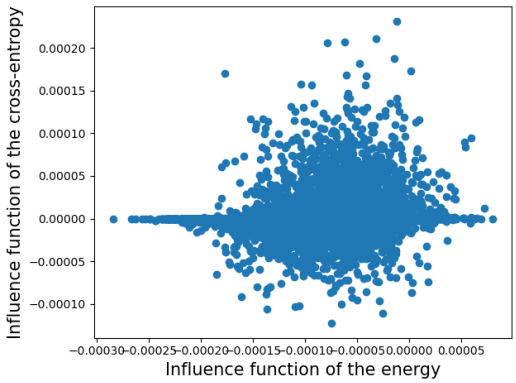

Figure 5: Relation between the influence of the cross-entropy and that of the energy. The influence is calculated for the ResNet-32 trained on CIFAR10 where each point represents a data sample.

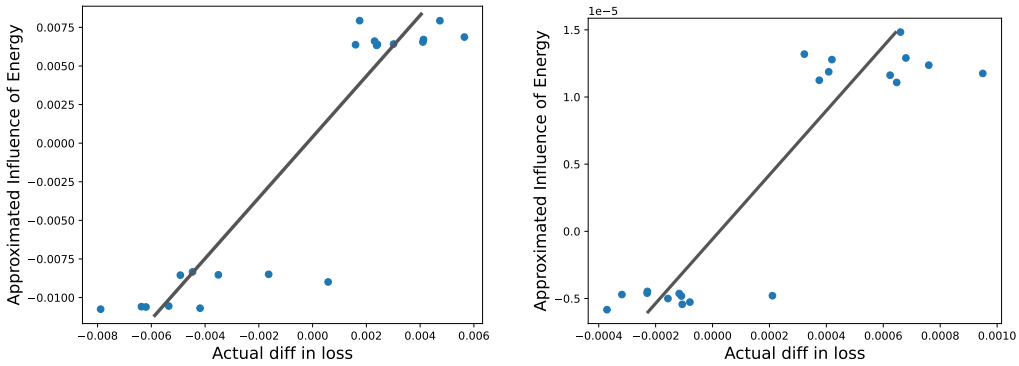

(a) ERM pre-trained model (Pearson's R $= 0.9154$) (b) LDAM pre-trained model (Pearson's R $= 0.9037$)

Figure 6: The positive relation between the calculated influence function and the actual change in testing loss on pre-trained CNN. We plot the top 20 most influential data points.

B Additional Experiment Results

B.1 Additional Results to Validate the Influence Function of Energy Regularization

In addition to Fig. 6, where we calculate the average influence over the whole testing set, we arbitrarily pick a wrongly classified data point and calculate its influence function following Koh & Liang (2017).

We calculate the influence function for the ResNet-32 trained with ERM on the long-tail CIFAR10 and long-tail CIFAR100, where the imbalance ratio is set to be 100. We plot the influence of energy regularization and the actual change in testing loss after finetuning the model with energy regularization for 50 epochs on 100 most influential data point. The calculated influence function has a positive relation to the actual change in loss (Pearson's R is 0.7875 on long-tail CIFAR10 and is 0.5744 on long-tail CIFAR100)

B.2 Energy Distribution Shifts During Training

We plot the energy distribution of the training set during the training of ResNet-32 by ERM on the long-tailed CIFAR10 with an imbalance ratio of 100. As shown in Fig. 7, the energy distribution keeps changing during the training even though the training loss is stable *e.g.* from 100-th epoch to 150-th epoch. We further plot the distribution at 160, 170, 180, 190, and 200 epochs after the learning rate has decayed. As shown in Fig. 7(b), the energy distribution of the training set still changes when the learning rate is decayed and the model is converged.

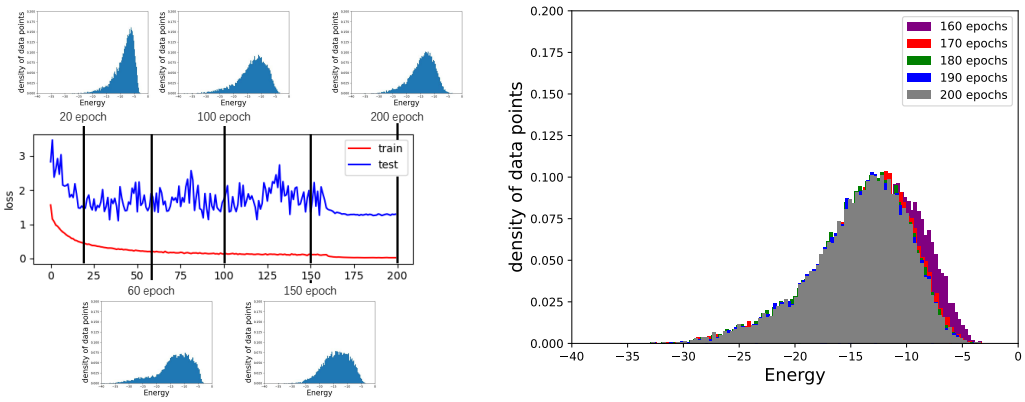

Figure 7: The energy distribution of a ResNet-32 trained on the long-tailed CIFAR10. (a): the energy distribution of the training set on different epochs during the training (b): the energy distribution of the training set at 160, 170, 180, 190, and 200 epoch.

Model	Dataset	iteration	repeat times	time used
ResNet-32	CIFAR10	5000	10	718.20s
ResNeXt-50	ImageNet-LT	1000	10	8492.92s
ResNet-152	iNaturalist 2018	1000	10	9701.74s

Table 7: Time required to approximate the influence function on different datasets for different models.

Method	Testing accuracy on different test domains(%)			
Colored MNIST	+80%	+90%	-90%	
ERM	72.3 ± 0.0	72.0 ± 0.1	10.1 ± 0.1	
ERM +IAER	73.8 ± 0.1	71.5 ± 0.1	10.6 ± 0.1	
PACS	A	C	P	S
ERM	85.6 ± 0.1	79.7 ± 0.2	98.9 ± 0.1	78.0 ± 0.1
ERM + IAER	84.2 ± 0.1	84.8 ± 0.1	97.3 ± 0.1	80.2 ± 0.1

Table 8: The detailed results for domain generalization where we report the testing accuracy(%) for different test domains.

B.3 Time Complexity Analysis

The main overhead of the proposed IAER is calculating the influence function of energy regularization. Since we approximate the influence function using stochastic approximation, the time used to calculate the influence function is determined by the choice of hyperparameters. We tested the time cost for calculating the influence function for ResNet-32 on CIFAR10 with Intel(R) Xeon(R) CPU E5-2678 v3 @ 2.50GHz and one GeForce RTX 2080Ti for 5000 iteration and averaged ten times. Approximating the influence function for a 5000 iteration takes 718.20s on average. As shown in Table B.3, we report the time used to approximate the influence function on different datasets for different models with the same hardware settings.

B.4 Detailed Results for Domain Generalization

We report the detailed results of our experiments for domain generalization, as shown in Table 8.

B.5 Proof for Remark 4.1

Proof. For the classifier $f_\theta : \mathbb{R}^D \to \mathbb{R}^K$, assume the energy on data point $\mathbf{x} \in \mathcal{R}^D$ is $E_\theta(\mathbf{x})$. For $\forall \mathcal{E} \in \mathcal{R}$, a classifier $g_\eta : \mathcal{R}^D \to \mathcal{R}^K$ could be defined that satisfies:

$$\forall i \in \{1, 2, \cdots, K\}, \quad g_\eta(\mathbf{x})[i] = f_\theta(\mathbf{x})[i]) - \mathcal{E} + E_\theta(\mathbf{x}). \tag{12}$$

By adding a certain value $E_\theta(\mathbf{x}) - \mathcal{E}$ to each logit $f_\theta(\mathbf{x})[i])$, the prediction of g_η is the same as the prediction of f_θ while the energy value of g_η is changed to $\mathcal{E}$.

For the predicted $\bar{p}_\eta(y|\mathbf{x})$ we have:

$$\begin{aligned}
\bar{p}_\eta(y|\mathbf{x}) &= \frac{\exp\left[f_\theta(\mathbf{x})[y]\right) - \mathcal{E} + E_\theta(\mathbf{x})]}{\sum_i \exp\left[f_\theta(\mathbf{x})[i]\right) - \mathcal{E} + E_\theta(\mathbf{x})]}, \\
&= \frac{\exp\left[f_\theta(\mathbf{x})[y]\right)]}{\sum_i \exp\left[f_\theta(\mathbf{x})[i])\right]}, \\
&= \bar{p}_\theta(y|\mathbf{x}).
\end{aligned} \tag{13}$$

For the energy $E_\eta(\mathbf{x})$ on the g_η, we have:

$$\begin{aligned}
E_\eta(\mathbf{x}) &= -\log \sum_i \exp\left[g_\eta(\mathbf{x})[i]\right] \\
&= -\log \sum_i \exp\left[f_\theta(\mathbf{x})[i] - \mathcal{E} + E_\theta(\mathbf{x})\right] \\
&= -\log \left(\exp[E_\theta(\mathbf{x}) - \mathcal{E}] \cdot \sum_i \exp\left[f_\theta(\mathbf{x})[i]\right] \right) \\
&= \mathcal{E} - E_\theta(\mathbf{x}) - -\log \sum_i \exp\left[f_\theta(\mathbf{x})[i]\right] \\
&= \mathcal{E} - E_\theta(\mathbf{x}) + E_\theta(\mathbf{x}) \\
&= \mathcal{E}.
\end{aligned} \tag{14}$$

□